Preparation and Characterization of Silver Sulfide Nanocrystals Generated from Silver(I)-Thiolate Polymers

T. Gregory Schaaff* and Adam J. Rodinone

Chemical Sciences Division, Oak Ridge National Laboratory, Oak Ridge, Tennessee 37831-6120

Received: April 11, 2003; In Final Form: May 30, 2003

Silver sulfide nanocrystals have been formed by the conversion of silver thiolate polymers with sodium sulfide in a dual-phase solution preparation. From transmission electron microscopy and laser desorption ionization mass spectrometry, the mean nanocrystalline diameter is estimated to be 5.4 nm. Large-angle X-ray diffraction is qualitatively consistent with the rhombic phase (acanthite) of Ag_2S. The removal of the silver thiolate polymer is confirmed by mass spectrometry, and initial results indicate that fractional crystallization may be utilized to separate these large nanocrystalline compounds by their respective core sizes. Optical absorption spectroscopy indicates a band gap of 1.1 eV, which is not shifted appreciably from the bulk value for this direct band gap semiconductor.

Introduction

Nanocrystalline compounds constitute a special class of nanostructured materials that can be manipulated in solutions, allowing for chemical analysis and separations. These emerging materials usually consist of small inorganic (metallic and nonmetallic) crystallites (tens to thousands of atoms) encapsulated by ligand molecules that are bound to the outermost layer of the nanocrystal, hence the colloquial monolayer-protected cluster compounds.[1] Silver sulfide nanocrystals have been synthesized by a number of methods. For example, Ag_2S nanocrystals have been formed in micelles[2−4] and from Ag(I)-glutathione complexes in aqueous solution.[5] Solid-phase conversion of silver suspended in polymers[6] and zeolites[7−9] has produced supported Ag_2S nanocrystals. These studies, combined with studies involving other metallic and semiconductor nanocrystalline compounds, have been instrumental in determining how electronic and chemical properties evolve when inorganic materials are confined to zero-dimensional systems on the nanometer scale.

A driving force behind the development of new chemical methods for preparing high-purity (size-selected) nanocrystalline compounds is the potential for "tuning" electronic properties of individual nanocrystals[10,11] and arrays assembled using nanocrystals.[12,13] Size-purified nanocrystalline compounds have aided in obtaining a fundamental understanding of how electronic and chemical properties evolve as a function of the inorganic nanocrystalline core (quantum size effects, QSEs) for both metallic[14] and semiconductor nanocrystals.[10] In semiconductor nanocrystalline compounds, QSEs are manifest spectroscopically in a widening of the band gap as the nanocrystalline core size is decreased and add discrete structure to absorption spectra in the case of direct band gap semiconductors (e.g., wurtzite CdSe).[15] However, an experimental determination of QSEs in metallic and semiconductor nanocrystals relies on the ability to produce highly uniform and well-defined nanocrystalline compounds (i.e., nanocrystals are of uniform size and the internal structure is single crystalline (on a per-nanocrystal basis)).[10]

Low-temperature preparations of silver sulfide typically produce α-Ag_2S (acanthite), which has monoclinic (rhombic) structure.[16] This phase is stable up to 177 °C, at which a phase transition occurs to form the cubic phase (argentite).[17,18] The optical properties of acanthite—a direct band gap semiconductor with a band gap of ∼1 eV—in thin films[19] and nanocrystals[6] are of special importance to solar, photographic, and near-IR photon-detection[20] devices. Despite the important prospects and the number of studies involving Ag_2S nanocrystals, few studies have addressed the near-IR optical properties of pure Ag_2S nanocrystals. For Ag_2S, Akamatsu and co-workers experimentally determined the band gap for Ag_2S nanocrystals with diameters of 4.7−11.2 nm and found that the band gap did not shift appreciably over this size range, indicating an absence of quantum confinement effects.[6] The quantity of Ag_2S nanocrystals that can be formed by the solid-phase conversion of silver is limited in many cases because loading supports too heavily causes the formation of much larger Ag and Ag_2S crystallites.

Solution-based preparations may be capable of producing larger quantities of Ag_2S nanocrystals provided that well-defined Ag-containing precursors that can be converted to stable forms of Ag_2S nanocrystalline compounds are identified. Reactions of silver ions with thiols result in the formation of silver(I)-thiolate polymers.[21] The polymers consist of six-membered rings of alternating Ag and S, with the thiolate tail group extending above and below the plane of the ring. Dance and co-workers have shown that in the solid form (with hydrophobic ligands) these polymers assemble into layered structures, which show intense peaks in low-angle X-ray scattering corresponding to the spacing between the "sheets" of the six-membered rings of Ag and S.[22]

One of the major hurdles to improving chemical methods for preparing nanocrystalline compounds lies in the ability to characterize nanocrystals *rapidly* and determine how slight changes in synthetic methods affect the final nanocrystalline product. Traditional materials characterization methods, such as TEM and X-ray diffraction, provide good information regarding the size, structure, and, in some cases, uniformity of nanocrystalline compounds, but these methods can be time-consuming and are not always amenable toward smaller

* Corresponding author. E-mail: schaaffg@ornl.gov. Phone: (865) 574-4878. Fax: (865) 576-8559.

10.1021/jp034979x CCC: $25.00
Published on Web 08/23/2003

nanocrystals (below ~2 nm). Below 2 nm, laser desorption ionization mass spectrometry (LDI-MS) provided a critical method for isolating gold nanocrystalline compounds.[23] Irradiating Au nanocrystalline films with high-intensity pulses of UV photons produced large fragment anions with masses corresponding to the approximate inorganic core composition of the gold nanocrystalline compound.[24,25] The speed at which mass spectra can be obtained (usually on the order of a few minutes) allows for efficient analyses of nanocrystalline samples generated under different conditions (e.g., changes in reaction parameters or separations by size).[26]

Here we report on the preparation of Ag_2S nanocrystals, which are formed by the conversion of silver(I)-dodecanethiolate polymers using Na_2S in a two-phase synthesis. In addition to transmission electron microscopy and X-ray diffraction, we show that laser desorption ionization mass spectrometry can be used to determine the approximate mass (or size) of the inorganic nanocrystalline core (i.e., Ag_2S without ligands). From mass spectrometric studies, initial results indicate that it may be possible to separate the Ag_2S nanocrystal by core size using fractional crystallization. Because the nanocrystals are in solution and can be concentrated easily without settling or agglomeration, we show that the band gap can be determined directly from near-IR optical absorption spectra.

Experimental Section

Synthesis of Ag_2S/SC12 Nanocrystalline Compounds. The synthesis of silver sulfide nanocrystals with dodecanethiolate ligands was performed under ambient conditions with a phase-transfer method similar to that used for the synthesis of gold[27] and silver[13] nanocrystalline compounds but using Na_2S instead of the reducing agent $NaBH_4$. The first step was the generation of the silver(I) polymer. Silver nitrate was dissolved in 50 mL of distilled and deionized water to a concentration of 20 mM. A separate organic solution was prepared by dissolving tetraoctylammonium bromide in 100 mL of toluene to a concentration of 40 mM. To the toluene solution, 1.5 mmol of dodecane thiol was added. With vigorous stirring, the aqueous solution was mixed with the organic solution. The two-phase mixture was stirred for an additional 30 min. If the two layers were mixed without the thiol present in the organic layer, then an appreciable amount of silver bromide formed, which impeded the formation of the Ag(I)-thiolate polymer. To the same stirring flask, 4.5 mL of a 100 mM aqueous solution of Na_2S was added. The organic (toluene) layer immediately changed from cloudy white/yellow to clear brown, indicating the formation of the nanocrystals. The solution was allowed to stir for an additional 12 h. Thus far, the quantities of the respective reagents and solvents have been increased by a factor of 5 (compared to those indicated above) with little or no change in the reaction products.

The two phases were separated in a separatory funnel, and the toluene solution was evaporated at 43 °C to ~3 mL using a rotary evaporator. To the concentrated solution, ethanol was added in excess to cause the precipitation of insoluble materials (nanocrystals and unreacted polymer starting material). The precipitate was filtered, dissolved, and reprecipitated typically five to six times to ensure the removal of all soluble starting materials (TOAB, thiol) and insoluble byproducts (Ag(I) SR polymer). Precipitation and filtration were continued until all of the precipitated material could be redissolved from the filter. That is, no material was visible on the filter after dissolving the brown precipitate. Following the repeated precipitations, attempts were made to separate the Ag_2S/SC12 nanocrystals by fractional crystallization (FC). FC was performed by placing a concentrated nanocrystalline solution (in toluene) inside a sealed desiccator with standing acetone. By stirring the nanocrystalline solution slowly, we found that vapor transfer of the acetone caused precipitation (usually overnight). The precipitate was removed with a 0.2-μm PTFE filter and then dissolved in toluene.

Transmission electron micrographs were obtained using a Hitachi HF-2000 cold field emission transmission electron microscope. Samples were prepared by dipping Holey carbon grids (Structure Probe, Inc.) into solutions of silver sulfide nanocrystals in toluene. The grids were dried under ambient conditions and placed directly into the microscope without further processing.

Laser desorption ionization mass spectrometry of the resulting material was performed on a modified R. M. Jordan (Grass Valley, CA) angular reflectron D-850 time-of-flight mass spectrometer. An additional detector assembly has been mounted behind the reflectron assembly to allow the mass spectrometer to operate in a linear time-of-flight mode. A frequency-tripled Nd:YAG laser was used to produce negative ions from films generated by drying 1 to 2 μL of concentrated solutions (10−15 mg/mL) on a stainless steel rod. Negative ions were accelerated to 1 keV upon desorption and detected using a conversion-dynode/microchannel plate detector assembly to provide an additional 20-keV post-flight acceleration. Although the use of a conversion dynode is an anathema to time-of-flight mass spectrometry because of losses in time resolution, we have found that it provides exceptional gains in intensity for high-mass ions, which have low velocities and produce weak ion-current signals on conventional (single-stage) detectors. Ion mass was calibrated by comparing the flight times of negative ions generated from MALDI of protein standards with large molecular weights (e.g., bovine transferrin, 78 030 Da; phosphorylase B, 138 973 Da). Because few calibration standards are available at high-mass range (>100 kDa), calibration was confirmed by comparing high-mass ions generated from gold nanocrystalline compounds, which can extend into the 200−700 kDa region.

XRD patterns are obtained in reflection mode from purified samples deposited as thick films (dried from toluene solutions) on miscut Si(111) wafers using Bruker Diffraction System D5005 (Cu Kα, $\lambda = 0.15405$ nm). Data were collected from 10 to 90° (2θ) in 0.025° steps with an acquisition time of 20 s at each step. Qualitative comparison to known bulk rhombic (acanthite) and cubic (argentite) phases of Ag_2S was performed using experimental diffraction patterns available from the ICSD database.

Optical absorption spectra were obtained using a Perkin-Elmer Lambda 19 UV−vis−NIR double-beam spectrophotometer. Dilute and concentrated solutions were prepared in hexane, and absorbance spectra were taken over the 2000−200 nm range.

Results

The reaction of Ag(I)SC12 polymers with Na_2S is best described as a degradation reaction because the formal charges of silver (1+) and sulfur (2−) presumably do not change in the formation of nanocrystals and the structure of the polymer is destroyed (i.e., not strictly a substitution reaction). The addition of Na_2S to the two-phase mixture caused an instantaneous color change from pale yellow (polymer) to dark brown (nanocrystals). As shown below, the reaction does not go to completion (i.e., polymeric silver remains even after 12-h reaction times). The polymer-to-nanocrystal conversion yield was estimated to be ~40% by recovering insoluble materials from the filter after the dissolution of nanocrystals at each precipitation step used

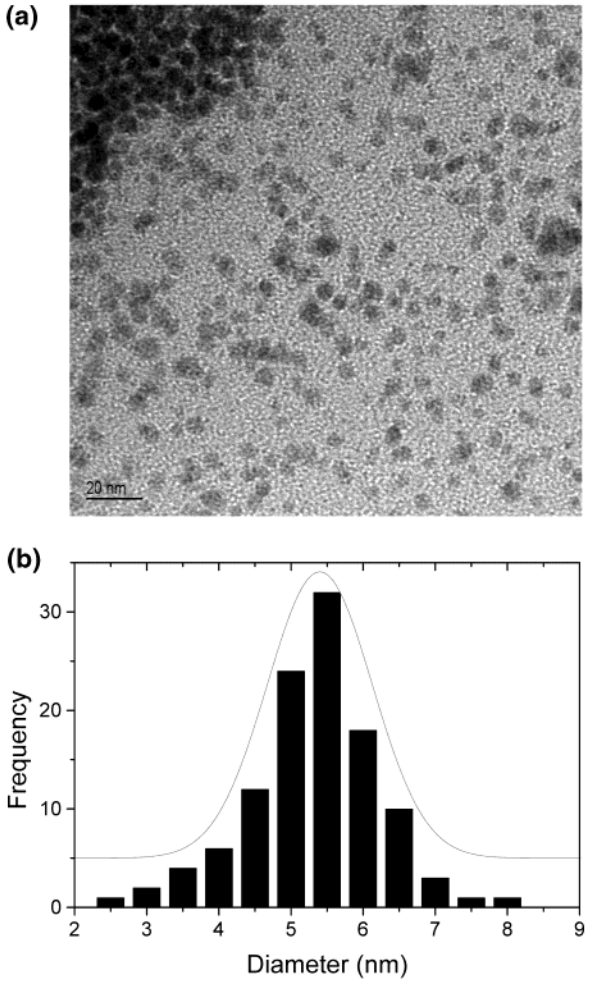

Figure 1. (a) Transmission electron micrograph of silver sulfide nanocrystals on a holey carbon grid. (b) Histogram of particle-size distribution for a and two similar micrographs taken at the same magnification.

to purify the nanocrystals. However, this is a crude estimate because small $[Ag(I)SC12]_n$ oligomers may have solubility characteristics similar to those of the nanocrystalline compounds. Reactions have been performed for 6, 12, and 24 h and show little effect on nanocrystalline sizes, as estimated by their respective ion abundances measured by LDI-MS. The amount of polymeric silver, however, does decrease from 6 to 12 h (by $\sim 1/3$) but shows less change from 12 to 24 h. The results below show the characterization of the purified silver sulfide dodecanethiolate (Ag_2S/SC12) nanocrystals by transmission electron microscopy, laser desorption ionization mass spectrometry, X-ray diffraction, and optical absorbance spectroscopy.

Electron Microscopy. After subsequent precipitations to remove all starting materials and byproducts of the reaction, a small amount of the brown solution containing the nanocrystals was applied to a holey carbon grid and allowed to dry under ambient conditions. Figure 1a shows transmission electron micrographs of an area having a high concentration of nanocrystals. Similar micrographs were used to generate a histogram of particle sizes (Figure 1b). The mean particle size (5.40 nm) and standard deviation (0.72 nm) are similar to those from previous reports of Ag_2S nanocrystals synthesized in micelles and capped with dodecanethiol.[2]

At higher resolution (Figure 2), fringes due to the Ag_2S lattice are visible in the nanocrystals. The spacing between adjacent fringes is consistent with the lattice spacing of Ag_2S thin film

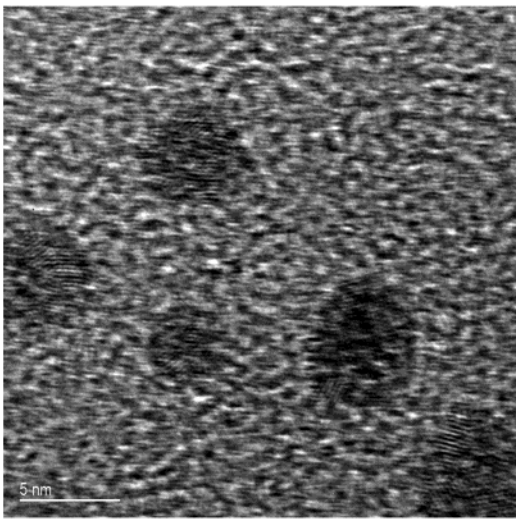

Figure 2. High-resolution transmission electron micrograph of individual nanocrystals. The measured lattice spacing is consistent with previous studies of silver sulfide nanocrystals and thin films.

solids[28] and other Ag_2S nanocrystals.[29] Thus far, the observed fringes indicate that the majority of the nanocrystals formed by these methods are not single crystallites. Each nanocrystal has a number of twinning planes depending on the size of the nanocrystals (i.e., larger nanocrystals are more twinned than smaller nanocrystals). This observation fits well with the extremely broad and nearly featureless X-ray diffraction pattern observed for the nanocrystals (see below).

Laser Desorption Ionization Mass Spectrometry. Laser desorption ionization mass spectrometry (LDI-MS) has been useful for determining the nanocrystalline core size for gold-thiolate nanocrystalline compounds by producing high-mass ions that correspond to the approximate mass of the gold core.[30] Figure 3 shows the LDI mass spectra from neat films of Ag_2S/SC12 nanocrystals after repeated precipitations. Because of the $\text{mass}^{-1/2}$ relationship with respect to time, the waveforms corresponding to ion flight times (shown in Figure 3) are plotted in μs (TOF) to facilitate the comparison of the abundances of anions detected with quite disparate masses. For this Figure, the corresponding masses are provided parenthetically in Figure 3 (in kDa) and in the text below.

The mass spectra of the Ag_2S/SC12 nanocrystals show three groups of peaks (Figure 3): (i) a group of peaks at times <100 μs ($\sim$3 kDa) having an adjacent peak spacing consistent with small $[Ag_NS_M]^-$ anions, (ii) a broad peak from 100 to 300 μs (3−10 kDa), and (iii) another broad peak from 500 to 1200 μs (100−600 kDa). Parts b and c of Figure 3show LDI mass spectra from neat films after the fourth and sixth precipitations, respectively. LDI-MS of the initial products (first two to three precipitations, Figure 3a) produced a high abundance of ions with flight times of less than 100 μs and an extremely low abundance of ions with longer flight times. It should be noted that high abundances of ions with short flight times can cause the saturation of the MCP detector, which deteriorates detector response from ions having longer flight times. Thus, relative ion abundances can be discriminatory toward ions with lower masses (shorter flight times). With successive precipitations, the abundance of peaks detected at times less than 300 μs decreased relative to the abundance of ions detected at times above 500 μs. The ion abundances detected at times above 500 μs (100 kDa) also showed weak but reproducible structure across this broad envelope of ions.

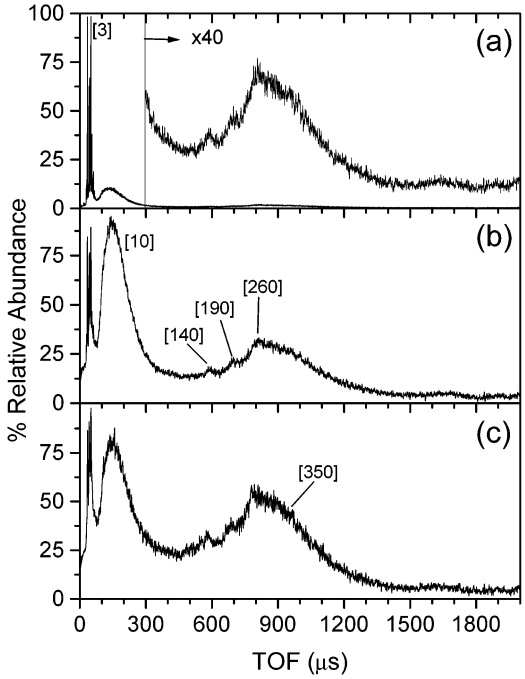

Figure 3. Laser desorption ionization time-of-flight mass spectra for the nanocrystalline products (after adding Na_2S) at various stages of polymer removal. The spectra were taken after the second, fourth, and sixth precipitations of nanocrystals from ethanol and are shown in a−c, respectively. The parenthetical labels correspond to the *m*/*z* value of the ions as determined by calibration with ions from proteins of known mass and large gold nanocrystals. Note the change in the abundance of ions arriving at short flight times (∼100 μs, 3 kDa) and longer flight times (∼800 μs, 260 kDa) after successive precipitations.

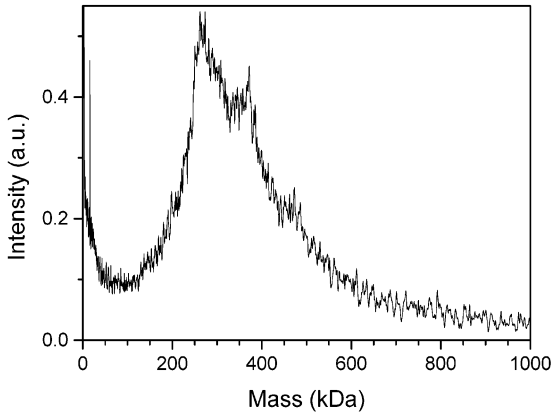

Figure 4. Laser desorption ionization time-of-flight mass spectrum for the first fraction obtained by fractional crystallization of the nanocrystalline product plotted in calibrated mass. Note the decrease in the abundance of ions at low mass and the suppression of the lower-mass ions visible in the TOF mass spectra of Figure 3.

Fractional crystallization (or size-selective precipitation) has been attempted with the Ag_2S/SC12 nanocrystals. Figure 4 shows the LDI mass spectrum corresponding to the first fraction separated from the sample shown in Figure 3c. This mass spectrum has been smoothed using a 15-point moving window average over the 25 000-point waveform and plotted in mass. The low-mass $[Ag_NS_M]^-$ anions were found to persist even after fractional crystallization and are off-scale in the Figure. After fractional crystallization, the intense, broad peak corresponding to ions in the 3−10 kDa (100−300 μs) range is not detected at the same relative abundance, compared to that of higher-mass ions. The two shoulders corresponding to ions having masses of 140 and 190 kDa are also suppressed but not completely removed. The mass spectrum shows slightly more pronounced peaks at 260 and 350 kDa than the mass spectrum obtained from the original mixture. In addition, a shoulder at 450 kDa appears that was not resolved in the original mixture.

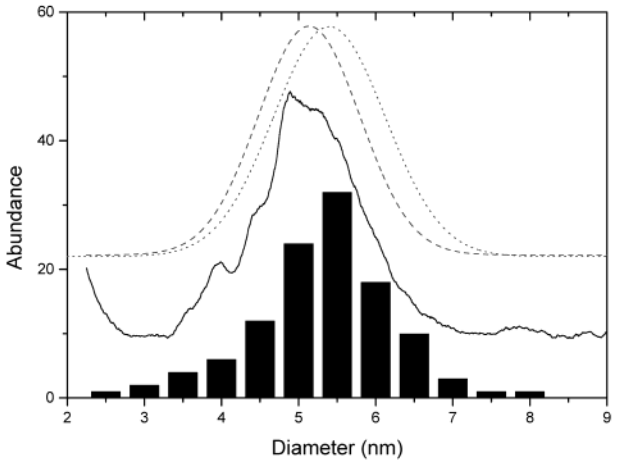

Figure 5. Overlay of the TEM histogram and the mass spectrum of Figure 3c comparing the two determinations of nanocrystalline size. The equivalent diameter of the mass spectrum was calculated using the bulk density of Ag_2S (acanthite) according to eq 1.

The relative ion abundances measured by mass spectrometry correlate well with the diameters determined by TEM. Figure 5 shows the mass spectrum from Figure 3c and the histogram generated from TE micrographs from the corresponding sample. The mean size and size distribution obtained by the two methods are similar. This mass spectrum was smoothed extensively (100-pt window) and baseline corrected so that an adequate fit to a Gaussian function could be obtained. The equivalent diameter (D_{eq}) of the mass measurement from LDI-MS can be easily calculated according to the equation

$$D_{eq} = \frac{N_{Ag_2S}}{\frac{\pi}{6} \cdot d} \quad (1)$$

where N_{Ag_2S} is the number of Ag_2S units in the ion (i.e., mass/247) and d is the bulk density of silver sulfide. The mean diameter obtained from the mass specturum was 5.13 ± 0.65 nm, compared to 5.40 ± 0.72 nm from the TEM histogram. The discrepancy in mean diameters derived from the two measurements is likely due to the combination of detector inefficiency at high mass in the mass spectrometer and the imaging quality of smaller nanocrystals.

X-ray Diffraction. Low-temperature preparations of Ag_2S are known to predominately form the rhombic phase, acanthite. The bulk wide-angle X-ray diffraction (WA-XRD) pattern of acanthite (ASTM standard 14-72, bars in Figure 6) is quite complex compared to that of the cubic phase (argentite), which forms in high-temperature (>177 °C) processes.[31] The measured WA-XRD pattern for the Ag_2S/SC12 nanocrystals (Figure 6) is qualitatively consistent with the bulk rhombic phase after considerating Scherrer broadening.[32] The cubic phase can be ruled out both from thermodynamic aspects and its inconsistency with the measured pattern. However, the pattern is not as well defined as would be expected for 4−5 nm particles (from TEM and LDI-MS). The high-resolution TE micrographs indicated that most Ag_2S/SC12 nanocrystals were not single crystalline but instead were composed of smaller single-crystal domains, which would be consistent with the rather featureless X-ray diffraction pattern.

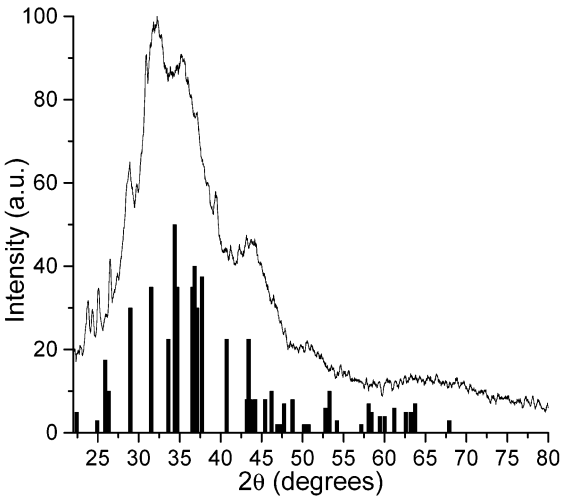

Figure 6. Large-angle X-ray diffraction pattern for the nanocrystals deposited on miscut Si(111). Although the rhombic phase of Ag_2S (calculated bulk pattern shown as bars) cannot be unambiguously assigned to these nanocrystals, the general form of the pattern does follow the expected intensity, assuming appreciable Scherrer broadening.

Although the presence of unreacted Ag(I)SR polymer can be inferred from the abundance of lower-mass ions in the mass spectra, X-ray diffraction data of films prepared from various samples confirmed its presence. Initial experiments (i.e., before our realization of polymer contamination) showed intense peaks in the small-angle region ($2\theta = 2-28°$) and are provided in Supporting Information. The positions of these peaks were generally consistent with known (layered) structures of Ag(I)SR polymers. The intensity of low-angle peaks decreased with successive precipitations, consistent with the lowering of abundant ions in the 3−10 kDa region of the mass spectra.

UV−Vis−NIR. The ability to concentrate solutions of nanocrystalline compounds allows for the extraction of electronic properties directly from the optical absorption spectra. Figure 7a shows the optical absorption spectrum for three solutions having concentrations of 0.475 and 4.75 mg/mL in hexane and 47.5 mg/mL Ag_2S/SC12 in hexane. By estimating the total molecular weight for the nanocrystals (i.e., Ag_2S core plus thiolate ligands) at ∼400 kDa, the molar absorption (extinction) coefficient is determined to be approximately 1×10^6 $M^{-1} \cdot cm^{-1}$ at 300 nm. The solutions were clear, and no settling of nanocrystals was observed, even in concentrated solutions. The silver-thiolate polymer (starting material) is transparent throughout the near-IR and visible regions of the spectrum. Solutions containing small, soluble oligomers show a broad absorption band starting at ∼6 eV, corresponding to the metal−ligand charge-transfer excitation. Two distinct features dominate the solution absorption spectra of the Ag_2S/SC12 nanocrystalline compounds: (i) a clear onset for optical absorption occurs at 1.1 eV (∼1100 nm) and (ii) an abrupt inflection occurs at 2.5 eV (∼500 nm).

The clear onset for absorption presumably corresponds to the band gap for the nanocrystalline compounds, which is not shifted significantly from the bulk value for α-Ag_2S. Although the optical absorption spectra obtained for Ag_2S/SC12 nanocrystals presented here and by others[2,5,6] are rather featureless, the derivative of one of the spectra (Figure 7b) shows features reminiscent of direct band gap semiconductor nanocrystals. However, the features observed here are not as discrete as those obtained for other direct band gap semiconductor nanocrystalline systems (e.g., size-selected CdSe).[33]

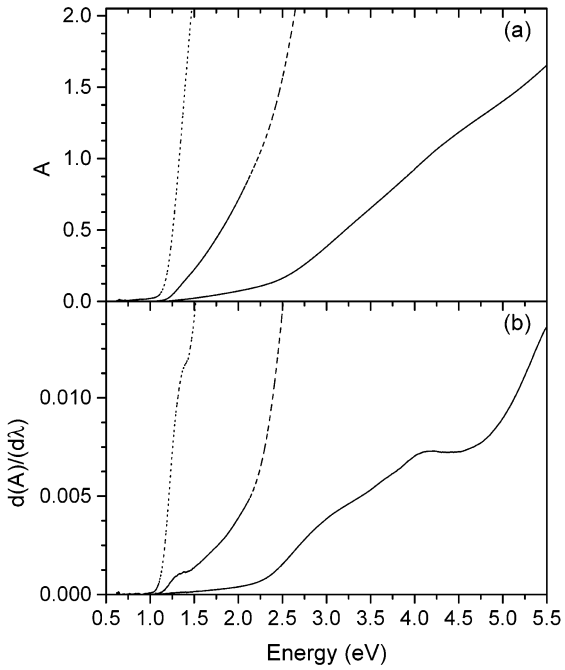

Figure 7. (a) Optical absorption spectra and (b) derivatives of spectra for three solutions having concentrations of 0.475 and 4.75 mg/mL in hexane and 47.5 mg/mL Ag_2S/SC12 in hexane. With the highest-concentration solution, the onset for optical absorption is determined to be 1.1 eV.

Discussion and Conclusions

Although the degradation of Ag(I)SC12 polymers by Na_2S clearly forms Ag_2S nanocrystals, the nanocrystalline quality and reaction yield are less than desirable. The reaction does not proceed to completion (i.e., the conversion of all Ag(I)SC12 to Ag_2S/SC12 nanocrystals). The isolation of nanocrystals from the starting materials, though, is achievable through repeated precipitation from toluene with ethanol. The removal of polymeric silver is confirmed by both mass spectrometry and X-ray diffraction measurements. Similar methods have been used to produce Ag_2S nanocrystals, but no indications of polymer contamination have been alluded to previously. In the case of glutathione-capped Ag_2S nanocrystals,[5] the bulky structure of glutathione presumably would likely prevent the formation of well-ordered layered structures, thus preventing the detection of these structures by X-ray diffraction methods.

As with gold nanocrystals, the application of LDI-MS to Ag_2S nanocrystals has proven helpful in many respects. The mass spectrometry is consistent with other, more time-consuming methods of analysis (e.g., size similar to TEM and polymer presence in X-ray diffraction). Mass spectra were obtained within minutes of each precipitation to confirm the removal of polymeric silver and indicate changes in ion abundances due to separations or reaction conditions. In addition, it provides support for the distribution determined by TEM. For the LDI-MS analysis, the ion detected abundances represent millions of ions produced by laser desorption ionization methods, not 100−200 particles (typical of TEM histograms). These studies have provided yet another benchmark for how mass spectrometry can be integrated into the characterization of nanocrystalline compounds. Although not a "stand-alone" technique, it provides a fast and easily automated method for nanocrystal analysis.

In the case of gold nanocrystals, under an intense pulse of UV radiation, gold nanocrystalline compounds desorb and fragment to form large anions with masses approximately equal

to that of the inorganic core of the nanocrystal.[24−26] For both gold and silver extended surfaces, the irradiation of thiolate monolayers with intense UV causes the selective cleavage of the S−C bond.[34,35] Because the mass spectrometry data were consistent with other measures of core size, it is likely that the high-mass ions form by a similar mechanism for the Ag_2S nanocrystalline compounds. For gold nanocrystals, the increased abundance of ions in specific regions of the mass spectra indicated special "islands of stability" or nanocrystalline compounds that were produced in higher abundance.[23] The mass spectra from the Ag_2S/SC12 nanocrystal also shows an enhancement in ion signals at 140, 190, 260, and 350 kDa. The detected ions would presumably correspond to extremely large nanocrystalline compounds having approximate inorganic core compositions of $Ag_{1100}S_{550}$, $Ag_{1500}S_{750}$, $Ag_{2000}S_{1000}$, and $Ag_{2800}S_{1400}$, respectively. However, confirming the presence of highly stable structures in this region will rely on the ability to separate these structures by size and further characterize each nanocrystalline compound.

With the evident importance of Ag_2S to solar, near-IR, and photographic applications, there seems to be a disparate amount of information regarding the optical properties of these nanocrystalline systems. Having the nanocrystals dissolved in solutions where concentrations can be readily changed without settling or agglomeration of the nanocrystals allows the determination of optical properties in a straightforward manner. For example, the band gap of 1.1 eV for these nanocrystals was determined directly from the absorption onset. This 1.1-eV band gap value is consistent with previous mathematical extraction from similarly sized Ag_2S nanocrystals suspended in a polymer matrix.[6]

As a direct band gap semiconductor, well-isolated (size-selected) Ag_2S nanocrystals would presumably have a highly structured optical absorption spectrum with intense bands. Structure in the optical absorption spectra of direct band gap semiconductors arises from the strongly allowed transitions due to selection rules. However, the optical absorption spectra shown here and reported by others appear somewhat featureless. The lack of structure is likely due to the broad distribution of nanocrystal sizes, evident in the LDI-MS and TEM. In addition, the poor crystallinity of the nanocrystalline cores, evident from TEM and X-ray diffraction measurements, likely causes the additional loss of discrete features in the spectra. It is well documented that spectral discreteness (observation of specific absorption bands) can deteriorate because of the overlap of absorption bands, which occur at different energies for nanocrystals having disparate sizes.[10] Because the nanocrystalline cores are not single-crystalline, electronically forbidden transitions may be allowed because of bonding that breaks symmetry and allows for vibronic excitations so that the optical spectra appear to be more similar to those of indirect band gap semiconductor nanocrystals.

Last, the initial goal of this research was to map out changes in the optical properties of Ag_2S nanocrystals in a size-dependent manner, similar to studies involving other direct band gap semiconductor nanocrystals. However, the Ag_2S/SC12 nanocrystals have not proven to be as amenable to size separations as other systems. Furthermore, the quality of the nanocrystals formed by the degradation of the Ag(I)SR polymers is not as desirable as expected (i.e., multiply twinned nanocrystals are predominant). Until now, few nanocrystalline systems (other than gold) have been studied using LDI-MS. The similarity of mass spectra for these Ag_2S nanocrystals and those obtained for gold nanocrystals suggests that similar types of large nanocrystalline systems may be studied in similar fashion, allowing for more efficient analyses to be performed for samples prepared under different reaction conditions or the monitoring of separations by size. Ongoing studies are considering methods to both improve the crystal structure of the nanocrystals (i.e., single-crystalline cores) and control the size of the nanocrystalline core through synthesis and separations.

Acknowledgment. We thank Professor Angus Wilkinson, Department of Chemistry at Georgia Tech for running the initial X-ray diffraction measurements and for insightful discussions regarding the experimental patterns. We also thank Laren Tolbert and Janusz Kowalik for use of the UV−vis−NIR instrumentation. Transmission electron micrographs were obtained at the Energy Efficiency and Renewable Energy User Facility of the High Temperature Materials Laboratory, Oak Ridge National Laboratory. This research was supported by the Laboratory Directed Research and Development Fund at Oak Ridge National Laboratory and the Division of Materials Sciences − Office of Basic Energy Sciences, U.S. Department of Energy at Oak Ridge National Laboratory, managed and operated by UT-Battelle, LLC under contract DE-AC05-00OR22725.

Supporting Information Available: Small- and wide-angle X-ray diffraction plots of products formed after the addition of Na_2S(aq) to the two-phase system containing silver(I) dodecanethiolate polymers. This material is available free of charge via the Internet at http://pubs.acs.org.

References and Notes

(1) Templeton, A. C.; Wuelfing, M. P.; Murray, R. W. *Acc. Chem. Res.* **2000**, *33*, 27−36.

(2) Pileni, M. P.; Motte, L.; Billoudet, F.; Mahrt, J.; Willig, F. *Mater. Lett.* **1997**, *31*, 255−260.

(3) Motte, L.; Pileni, M. P. *J. Phys. Chem. B* **1998**, *102*, 4104−4109.

(4) Motte, L.; Pileni, M. P. *Appl. Surf. Sci.* **2000**, *164*, 60−67.

(5) Brelle, M. C.; Zhang, J. Z.; Nguyen, L.; Mehra, R. K. *J. Phys. Chem. A* **1999**, *103*, 10194−10201.

(6) Akamatsu, K.; Takei, S.; Mizuhata, M.; Kajinami, A.; Deki, S.; Takeoka, S.; Fujii, M.; Hayashi, S.; Yamamoto, K. *Thin Solid Films* **2000**, *359*, 55−60.

(7) Bruhwiler, D.; Seifert, R.; Calzaferri, G. *J. Phys. Chem. B* **1999**, *103*, 6397−6399.

(8) Bruhwiler, D.; Leiggener, C.; Glaus, S.; Calzaferri, G. *J. Phys. Chem. B* **2002**, *106*, 3770−3777.

(9) Calzaferri, G.; Bruhwiler, D.; Glaus, S.; Schurch, D.; Currao, A.; Leiggener, C. *J. Imaging Sci. Technol.* **2001**, *45*, 331−339.

(10) Murray, C. B.; Norris, D. J.; Bawendi, M. G. *J. Am. Chem. Soc.* **1993**, *115*, 8706−8715.

(11) Schaaff, T. G.; Shafigullin, M. N.; Khoury, J. T.; Vezmar, I.; Whetten, R. L.; Cullen, W. G.; First, P. N.; Gutierrez, C.; Ascensio, J.; Jose-Yacaman, M. J. *J. Phys. Chem. B* **1997**, *101*, 7885−7891.

(12) Motte, L.; Billoudet, F.; Lacaze, E.; Douin, J.; Pileni, M. P. *J. Phys. Chem. B* **1997**, *101*, 138−144.

(13) Heath, J. R.; Knobler, C. M.; Leff, D. V. *J. Phys. Chem. B* **1997**, *101*, 189−197.

(14) Chen, S.; Ingram, R. S.; Hostetler, M. J.; Pietron, J. J.; Murray, R. W.; Schaaff, T. G.; Khoury, J. T.; Alvarez, M. M.; Whetten, R. L. *Science* **1998**, *280*, 2098−2101.

(15) Alivisatos, A. P. *J. Phys. Chem.* **1996**, *100*, 13226−13239.

(16) Sadanaga, R.; Sueno, S. *Miner. J. (Japan)* **1967**, *5*, 124−131.

(17) Cava, R. J.; Reidinger, F.; Wuensch, B. J. *J. Solid State Chem.* **1980**, *31*, 69−78.

(18) Cava, R. J.; McWhan, D. B. *Phys. Rev. Lett.* **1980**, *45*, 2046−2048.

(19) Bennett, J. M.; Stanford, J. L.; Ashley, E. J. *J. Opt. Soc. Am.* **1969**, *59*, 499.

(20) Kitova, S.; Eneva, J.; Panov, A.; Haefke, H. *J. Imaging Sci. Technol.* **1994**, *38*, 484−488.

(21) Dance, I. G. *Polyhedron* **1986**, *5*, 1037−1104.
(22) Dance, I. G.; Fisher, K. J.; Banda, R. M. H.; Scudder, M. L. *Inorg. Chem.* **1991**, *30*, 183−187.
(23) Whetten, R. L.; Khoury, J. T.; Alvarez, M. M.; Murthy, S.; Vezmar, I.; Wang, Z. L.; Stephens, P. W.; Cleveland, C. L.; Luedtke, W. D.; Landman, U. *Adv. Mater.* **1996**, *8*, 428−433.
(24) Vezmar, I.; Alvarez, M. M.; Khoury, J. T.; Salisbury, B. E.; Shafigullin, M. N.; Whetten, R. L. *Z. Phys. D* **1997**, *40*, 147−151.
(25) Arnold, R. J.; Reilly, J. P. *J. Am. Chem. Soc.* **1998**, *120*, 1528−1532.
(26) Schaaff, T. G.; Shafigullin, M. N.; Khoury, J. T.; Vezmar, I.; Whetten, R. L. *J. Phys. Chem. B* **2001**, *105*, 8785−8796.
(27) Brust, M.; Walker, M.; Bethell, D.; Schiffrin, D. J.; Whyman, R. *J. Chem. Soc., Chem. Commun.* **1994**, 801−802.
(28) Aragonsantamaria, P.; Santosdelgado, M. J.; Maceiravidan, A.; Polodiez, L. M. *J. Mater. Chem.* **1991**, *1*, 409−413.
(29) Shiozawa, T.; Kobayashi, T. *Phys. Status Solidi A* **1988**, *110*, 375−382.
(30) Whetten, R. L.; Shafigullin, M. N.; Khoury, J. T.; Schaaff, T. G.; Vezmar, I.; Alvarez, M. M.; Wilkinson, A. *Acc. Chem. Res.* **1999**, *32*, 397−406.
(31) MeherziMaghraoui, H.; Dachraoui, M.; Belgacem, S.; Buhre, K. D.; Kunst, R.; Cowache, P.; Lincot, D. *Thin Solid Films* **1996**, *288*, 217−223.
(32) Klug, H. P.; Alexander, L. E. *X-ray Diffraction Procedures for Polycrystalline and Amorphous Materials*, 2nd ed.; Wiley-Interscience: New York, 1974.
(33) Alivisatos, A. P. *Science* **1996**, *271*, 933−937.
(34) Kondoh, H.; Nozoye, H. *J. Phys. Chem. B* **1998**, *102*, 2367−2372.
(35) Lewis, M.; Tarlov, M.; Carron, K. *J. Am. Chem. Soc.* **1995**, *117*, 9574−9575.